Proton-coupled electron transfers in biomimetic water bound metal complexes. The electrochemical approach†

Elodie Anxolabéhère-Mallart,[a] Cyrille Costentin,[a] Clotilde Policar,[b] Marc Robert,*[a] Jean-Michel Savéant[a] and Anne-Lucie Teillout[a]

Received 15th March 2010, Accepted 28th April 2010
DOI: 10.1039/c004276e

Water-bound metal (M) complexes play a central role in the catalytic centers of natural systems such as Photosystem II (PSII), superoxide dismutase, cytochrome c oxidase and others. In these systems, electron transfer reactions involving the metal center are coupled to proton transfers. Besides its fundamental interest, comprehension of these reactions and of possible bio-inspired catalytic devices is an additional motivation for studying the coupling between proton and electron transfer (proton-coupled electron transfers, PCET), starting with an aqua-M^{II}/hydroxo-M^{III} couple, and going to higher oxidation degrees as in the case of PSII (hydroxo-M^{III}/oxo-M^{IV} couple). Factors that determine the occurrence of the stepwise and concerted pathways are recalled from the illustrating example of a recently described mononuclear osmium complex, thus opening perspectives for further studies of the biomimicking complex. PCET in a mononuclear aqua/hydroxo manganese couple was then studied using the electrochemical approach.

Introduction

Proton coupled electron transfer (PCET) reactions play a critical role in a variety of biological and chemical processes.[1] Prominent examples, among others, such as Photosystem II,[2–4] superoxide dismutase (SOD)[5–7] or cytochrome c oxidase,[8] involve proton-coupled electron transfer reactions in metal complexes, playing an essential role in the succession of steps leading to catalysis of the reaction. The remarkable efficiency of these enzymatic systems could lie in the fact that proton and electron transfers are so intimately coupled that they are in fact concerted.[4] As a consequence, unraveling the mechanisms of proton-coupled electron transfers is an important task from a fundamental viewpoint, but also in order to design and elaborate efficient biomimetic complexes, all along nature guidelines. Active attention is thus currently devoted to the competition between the possible pathways.[9]

The stepwise pathways (grey pathways in Scheme 1) involve separated steps for proton and electron transfer. These stepwise pathways form a square reaction scheme in which electron transfer is followed by proton transfer (EPT pathway)

[a]*Laboratoire d'Electrochimie Moléculaire, Unité Mixte de Recherche Université - CNRS No 7591, Université Paris Diderot, Bâtiment Lavoisier, 15 rue Jean de Baïf, 75205 Paris Cedex 13, France. E-mail: robert@univ-paris-diderot.fr; Fax: +33 1 57 27 87 88; Tel: +33 1 57 27 87 90*
[b]*Laboratoire des BioMolécules, UMR 7203, UPMC, Département chimie de l'ENS, 24 rue Lhomond, 75231 Paris Cedex 05, France*

† Electronic supplementary information (ESI) available: Further theoretical and experimental details. See DOI: 10.1039/c004276e

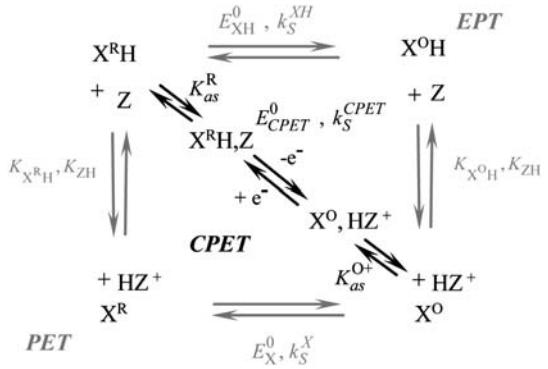

Scheme 1 Pathways for PCET oxidation. The superscripts O and R stand for "oxidized" and "reduced", respectively. Z (charge not shown)/HZ^+ is any electroinactive acid–base couple.

or proton transfer is followed by electron transfer (PET pathway). In the concerted pathway, proton and electron transfer are transferred in a single step (black pathway, Scheme 1), thus avoiding the high energy intermediates encountered along the two steps mechanisms. It may involve prior formation of an adduct combining the reactant with the proton accepting species Z (*e.g.* the base of a buffer if the reaction takes place in buffered water), as shown in Scheme 1. After the concerted proton–electron transfer (CPET) has taken place within this adduct, the reaction may or may not go through the intermediacy of an adduct before the oxidized species is finally formed.

When electronic steps are rate determining, the reaction scheme can be described as an apparent electron transfer. Its thermodynamic is determined by an apparent potential which can be related to the standard potentials characterizing each pathway E^0_{XH}, E^0_X and E^0_{CPET} for the EPT, PET and CPET pathways, respectively, according to eqn (1) and (2). Eqn (2) was obtained by considering, as is more often the case, that association constants between the complex (oxidized or reduced form respectively) and the buffer components (acid or base respectively) are weak and about the same. The apparent standard potential is currently related to the pH by the classical Pourbaix diagram (Fig. 1).

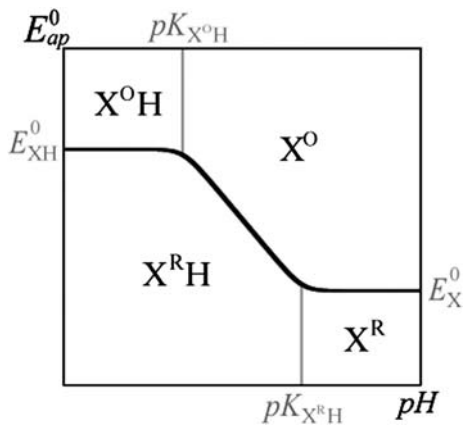

Fig. 1 Pourbaix diagram showing the variation of the apparent standard potential E^0_{ap} with pH and the characteristic pK values and standard potentials.

$$E^0_{ap} = E^0_{XH} + \frac{RT}{F}\log\left(\frac{[H^+] + K_{X^RH}}{[H^+] + K_{X^OH}}\right) = E^0_X + \frac{RT}{F}\log\left(\frac{K_{X^OH}}{K_{X^RH}}\frac{[H^+] + K_{X^RH}}{[H^+] + K_{X^OH}}\right) \quad (1)$$

$$E^0_{ap} = E^0_{CPET} + \frac{RT}{F}\log\left(\frac{K_{X^OH}}{K_{ZH}}\frac{[H^+] + K_{X^RH}}{[H^+] + K_{X^OH}}\right) \quad (2)$$

Whether the mechanism is stepwise or concerted, the kinetic law that relates the current density, I, to the electrode potential, E, can be approximated by the linear Butler–Volmer eqn (3) (in the experimental conditions usually encountered a value of the apparent transfer coefficient equal to 0.5 could be used, provided that all acid–base and association/dissociation reactions in Scheme 1 are so fast as to remain at equilibrium, the [ ]'s being the concentrations of oxidant and reductant at the electrode surface).[9,10]

$$\frac{I}{F} = k^{ap}_S \exp\left[\frac{F}{2RT}(E - E^0_{ap})\right]\left(\sum[red] - \sum[ox]\exp\left[-\frac{F}{RT}(E - E^0_{ap})\right]\right) \quad (3)$$

The apparent electronic transfer kinetic is characterized by an apparent standard rate constant k^{ap}_S which represents the common value of the oxidation and reduction rate constants when the electrode potential is set at a value equal to the apparent standard potential, E^0_{ap}. Its "apparent" character refers to the fact that it does not represent an elementary step but it is a combination of standard rate constants characterizing each intervening pathway. In other words, the PCET mechanism results from the competition between stepwise and concerted apparent kinetic contribution. With reference to Scheme 1, the apparent standard rate constant may be expressed as the sum of the various standard rate constants (k^X_S, k^{XH}_S and k^{CEPT}_S for the PET, EPT and CPET pathways respectively), each of them being weighted by the contribution of the corresponding pathway, thus leading to eqn (4).[10] In this equation, K^{O+}_{as} and K^R_{as} represent the association constants as defined on Scheme 1.

$$k^{ap}_S = \frac{k^X_S}{\sqrt{1 + \frac{[H^+]}{K_{X^OH}}}\sqrt{1 + \frac{[H^+]}{K_{X^RH}}}} + \frac{k^{XH}_S}{\sqrt{1 + \frac{K_{X^OH}}{[H^+]}}\sqrt{1 + \frac{K_{X^RH}}{[H^+]}}} + \frac{k^{CPET}_S\sqrt{K^{O+}_{as}K^R_{as}}\sqrt{[HZ^+][Z]}}{\sqrt{1 + \frac{[H^+]}{K_{X^OH}}}\sqrt{1 + \frac{K_{X^RH}}{[H^+]}}} \quad (4)$$

Successive oxidations of transition metal aqua complexes, starting at the two-oxidation state, $M^{II}(OH_2)$ to $M^{III}(OH)$, then to $M^{IV}(O)$ and possibly $M^{V}(O)$, is a domain where PCET reactions are very common, as can be read from the many Pourbaix diagrams that have been recorded.[11,12] Indeed, proton transfer allows us to avoid charge accumulation upon successive redox events thus leveling off

oxidation potentials. The mechanism of these PCET reactions—concerted or stepwise—is an important issue in the understanding of natural systems and design of artificial systems catalyzing the formation of dioxygen from the $4e^-$ oxidation of water, as well as the dismutation of the superoxide anion into dioxygen and hydrogen peroxide within cells, for example.[5–7] The mechanism of the PCET oxidation of $M^{II}(OH_2)/M^{III}(OH)/M^{IV}(O)$ PCET sequence has been addressed in pioneering electrochemical and homogeneous studies of ruthenium complexes.[13–16] The mechanistic analysis was however incomplete and additionally obscured by the possible interference of $Ru^{II} + Ru^{IV}$ disproportionation. The domain of thermodynamic existence of the Ru^{III} is indeed very narrow over the accessible range of pH. This drawback can be bypassed with osmium complexes which present larger thermodynamic existence domains. Electrochemical kinetic studies have been previously performed in details for two osmium complexes: $[Os^{II}(bpy)_2(4\text{-Npy})(H_2O)]^{2+}$ (4-Npy = 4-aminopyridine)[17,18] and $[Os^{II}(bpy)_2py(H_2O)]^{2+}$ (py = pyridine, bpy = 2,2′-bispyridine, Scheme 2).[11,19] They lead to firm conclusions as concerns the oxidation mechanisms, and allowed to underscore the general factors controlling the reactivity. The main parameters are hereafter recalled and guidelines for further studies are proposed. The validity of the assumption commonly made for PCET processes in buffered aqueous media that all acid–base reactions remain at equilibrium is discussed. Manganese complexes aiming at mimicking catalytic centers of biological centers (PSII, SOD, catalase) have also been described although no mechanistic analysis of the PCET reaction involving the redox chemistry of Mn is available. A major drawback is that electrochemical study of such complexes is often obscured by formation of manganese polynuclear species and/or adsorption onto the electrode surface.[20–23] We took the example of a Mn-SOD mimicking complex for analyzing the proton-coupled electron transfer in Mn^{II}-aqua/Mn^{III}-hydroxo couple in buffered aqueous media. Several difficulties have been encountered leading to the impossibility to get a firm conclusion regarding mechanism but allowing to provide indication for improvement of the mimicking system.

Results and discussion

Three main experimental criteria allow discrimination between a stepwise and a concerted pathway. One involves the fitting of the apparent standard rate constant variation with pH, using eqn (4), provided that intrinsic kinetic and thermodynamic parameters are known or could be bracketed with a good accuracy. Secondly,

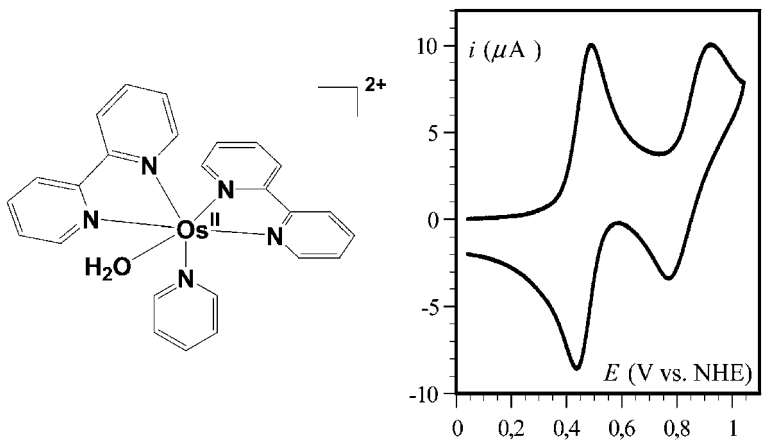

Scheme 2 Cyclic voltammetry of $[Os(bpy)_2py(H_2O)]^{2+}$ in Britton–Robinson buffer (pH = 3, 0.1 M) at a boron-doped diamond electrode.

a description using only the contributions from stepwise pathways would be a first strong indication that the reaction proceeds in two steps. The measure of a significant kinetic isotope effect is characteristic of a concerted mechanism because it is the only one to admit a proton transfer in its rate determining step. While it is assumed here that proton transfers are at equilibrium because reactions take place in buffered water, one may wonder whether this assumption is always fulfilled and argue that, if not, a kinetic isotope effect would not be characteristic of a concerted mechanism. This point will be discussed in section 1 and it will be shown that it is possible to distinguish between sequential and concerted mechanisms. The third mechanistic clue is offered by the possible buffer concentration dependence of the apparent standard rate constant. As shown by eqn (4), the concerted contribution is proportional to the square root of each buffer component concentration. The use of all three criteria (electron transfer kinetics, kinetic isotope effect and buffer concentration effect) over a sufficiently large pH range usually allows a conclusion regarding the PCET mechanism. It has been demonstrated within this framework that the $Os^{II}(H_2O)$ ($[Os^{II}(bpy)_2(4\text{-}Npy)(H_2O)]^{2+}$) oxidation into the $Os^{III}(OH)$ complex, with the molecules being attached to long-chain thiols self-assembled onto a gold surface, is a concerted pathway.[17,18] In contrast, kinetic studies of the $[Os^{II}(bpy)_2py(H_2O)]^{2+}$ complex (Scheme 2) in freely diffusing conditions and in buffered aqueous media at glassy carbon (Os^{II}/Os^{III}) and boron-doped diamond (Os^{III}/Os^{IV}) electrodes, have allowed to conclude that it involves a stepwise $Os^{II}(OH_2)/Os^{III}(OH)$ transfer and a concerted $Os^{III}(OH)/Os^{IV}(O)$ transfer.[11,19] This study is the first one that demonstrates the occurrence of a concerted PCET reaction involving metal transition complexes. The generality and significance of the factors controlling the mechanism will be recalled in section 1 and validity of the assumption made for that all acid–base reactions remain at equilibrium will be discussed. From these guidelines, a first attempt to extend our electrochemical approach to a $Mn^{II}(OH_2)/Mn^{III}(OH)$ couple, opening the way to the study of highly oxidized, catalytically active manganese complexes, is presented in section 2.

1. Controlling factors in PCET oxidations involving metal complexes

Thermodynamics of PCET process (Scheme 1) depends on two acidity constants, K_{X^RH} and K_{X^OH}, related to two acid–base couples, X^RH/X^R for the reduced species and X^OH/X^O for the oxidised species (Scheme 1). From eqn (4), it appears that the apparent standard rate constant also depends on these acidity constants. Simulations have been performed for various acidity constant values in buffered solutions

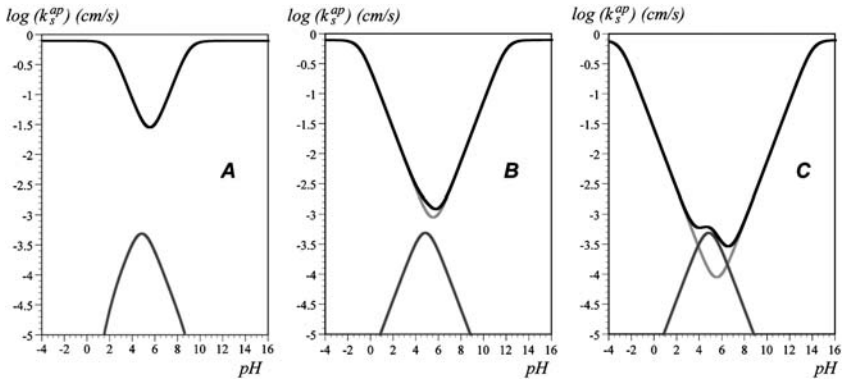

Fig. 2 Variation of the apparent standard rate constant with pH, as a function of the pK_a gap between the redox states (A: p$K_{X^RH} = 9$ and p$K_{X^OH} = 2$, B: p$K_{X^RH} = 12$ and p$K_{X^OH} = -1$, C: p$K_{X^RH} = 14$ and p$K_{X^OH} = -3$). Black line: apparent standard rate constant, light grey: stepwise pathway contribution, dark grey: concerted pathway contribution. [Z] + [HZ$^+$] = 0.1 M, pK_a(HZ$^+$/Z) = 5. $k_S^X = k_S^{XH} = 0.8$ cm s^{-1} and $k_S^{CEPT}\sqrt{K_{as}^{O+}K_{as}^{R}} = 0.01$ cm s^{-1} M^{-1}.

and taking typical intrinsic electron transfer,[19] showing the different contributions to the apparent standard rate constant (Fig. 2). For the sake of simplicity, only one buffer couple (HZ^+/Z with a pK_a of 5) is considered to be able to undergo a concerted mechanism. It can be seen that the larger the pK_a gap ($pK_{X^RH} - pK_{X^OH}$), the higher in energy the reaction intermediates of the sequential routes (therefore the formation of X^R and X^OH becomes less favourable, Scheme 1), and the more important the concerted (CPET) contribution is. Studies of the couples $Os^{II}(OH_2)/Os^{III}(OH)$ and $Os^{III}(OH)/Os^{IV}(O)$ ($[Os^{II}(bpy)_2py(H_2O)]^{2+}$ complex) provide relevant illustrative examples.[11,19] Note that for both couples it was possible to fit the rate constant for electron transfer, with the theoretical variation using eqn (4), along the whole range of pH investigated. For the $Os^{II}(OH_2)/Os^{III}(OH)$ couple, the pK_a involved are close enough one from the other ($pK_{X^RH} = 9.1$ and $pK_{X^OH} = 2$) for the mechanism to be stepwise, thus confirming that a small pK_a gap involves energetically inexpensive reaction intermediates and contains a negligible concerted contribution (this case corresponds to Fig. 2A). For the $Os^{III}(OH)/Os^{IV}(O)$ couple, it was not possible to determine the acidic constants from the Pourbaix diagram, and the pK_a gap could thus be assumed being higher than 14.[19] In this case, the reaction follows a concerted (CPET) pathway. This corresponds to the Fig. 2C case where a large pK_a gap leads to an important concerted contribution in a pH range close to the buffer pK_a. Nevertheless, it should be kept in mind that the more important pK_a gap is, the smaller the apparent standard rate constant is (for a given intrinsic standard rate constant). Thereby, the CPET pathway has a thermodynamic advantage but it involves slower intrinsic kinetics.

As mentioned previously, it is worth questioning the assumption of having proton transfers at unconditional equilibrium when the pK_a gap is large. When either the pK_a of the reduced state is very high (*e.g.* higher than 14) or the pK_a of the oxidized state is very low (*e.g.* negative), the corresponding equilibrium constant for proton transfer (PET pathway in the first case and EPT pathway in the second case) are respectively very small or very large (eqn (5)) at intermediate pH (we assume here that the buffer pK_a is equal to the considered pH):

$$K_{PT}^{PET} = 10^{pH-pK_{X^RH}},\ K_{PT}^{EPT} = 10^{pH-pK_{X^OH}} \tag{5}$$

A complete formal description of both PET and EPT mechanism (respectively named CE and EC mechanisms in the general case of a first order coupled chemical reaction with electron transfer) has been done a few decades ago.[24,25] It has been shown that in both cases, and assuming fast electron transfer, the kinetic regime depends upon two parameters, the equilibrium constant and a kinetic parameter $\lambda = \frac{RT}{F}\frac{k_p^{ap} + k_{-p}^{ap}}{v}$ (with $K_{PT}^{PET \text{ or } EPT} = k_p^{ap}/k_{-p}^{ap}$), v is the scan rate while k_p^{ap} and k_{-p}^{ap} are the apparent deprotonation and protonation rate constants, respectively. If proton transfer is controlled by diffusion in the down-hill direction, then $\lambda \approx \frac{RT}{F}\frac{k_{dif}[Z]}{v}$, where $[Z]$ is half of the total buffer concentration and k_{dif} is the diffusion limit. Provided that $\log \lambda > 2$, which is achieved at typical scan rate and buffer concentration used, it can be deduced from zone diagrams (see ESI†) that the transition between the so-called DE zone (corresponding to proton transfer being at equilibrium) and the KE zone (corresponding to interference of the proton transfer step in the kinetics) occurs when $\log K_{PT}^{PET} = 0.75 - 0.5\log \lambda$, *i.e.* for $pH < pK_{X^RH} + 0.75 - 0.5\log\left(\frac{RT}{F}\frac{k_{dif}[Z]}{v}\right)$ in the PET case, and when $log\ K_{PT}^{EPT} = -0.75 - 0.5\log \lambda$, *i.e.* for $pH > pK_{X^OH} - 0.75 + 0.5\log\left(\frac{RT}{F}\frac{k_{dif}[Z]}{v}\right)$ in the EPT case. Moreover, assuming that the electron transfer steps involved in the stepwise pathways have comparable standard rate constants, it can be seen from eqn (4)

that the EPT pathway prevails when $pK_{X^OH} < pH < \frac{pK_{X^OH} + pK_{X^RH}}{2} - 1$ while the PET pathway prevails when $\frac{pK_{X^OH} + pK_{X^RH}}{2} + 1 < pH < pK_{X^RH}$. We can thus conclude that proton transfer can be considered at equilibrium on the whole pH range if:

$$pK_{X^RH} - pK_{X^OH} < 0.5 + \log\left(\frac{RT}{F}\frac{k_{dif}[Z]}{v}\right) \quad (6)$$

This criterion shows that for systems with a large pK_a gap the relative weight of the concerted pathway as compared to the relative weight of stepwise pathways can be even more important than predicted from eqn (4). In such cases, the shape of the voltammograms may deviate from simple apparent monoelectronic wave and kinetic analysis has to be considered carefully.

The condition given through eqn (6) is fulfilled in the case of the $Os^{II}(OH_2)/Os^{III}(OH)$ couple (taking $k_{dif} = 10^{10}$ M^{-1} s^{-1}, $v = 0.2$ V s^{-1} and $[Z] = 0.05$ M). As mentioned previously, with the $Os^{III}(OH)/Os^{IV}(O)$ couple, while it is not known for certain, a larger pK_a gap is expected and the above condition is probably no more fulfilled in the experimental conditions. However, considering on one hand the EPT stepwise pathway, anodic peak potential is expected to be more positive than the one obtained for a proton transfer being at equilibrium, and the chemical reversibility of the wave starts to decrease (see ESI†). These criteria can be easily used to rule out or validate the EPT pathway in this regime where the kinetic isotope effect is no more discriminating (when proton transfers are at unconditional equilibrium, a kinetic isotope effect is a signature of a concerted reaction). On the other hand, considering the PET stepwise pathway, the anodic peak current is expected to decrease while a new more positive peak appears (see ESI†). Again, these criteria can be used to rule out or validate the PET pathway.

As can be seen from both eqn (4) and Scheme 1, the buffer plays a crucial role in the competition between stepwise and concerted pathways. It appears from the mathematical expression of eqn (4) that the more concentrated the buffer, the stronger the contribution of the CPET is. Fig. 3 shows the variation of the apparent standard rate constant with pH, as a function of the buffer concentration. Again, for the sake of simplicity, only one buffer couple (HZ^+/Z with a pK_a of 5) is considered to be able to undergo a concerted mechanism. For the highest buffer concentration used (5 M), the simulation shows a clear CPET contribution (Fig. 3C). The

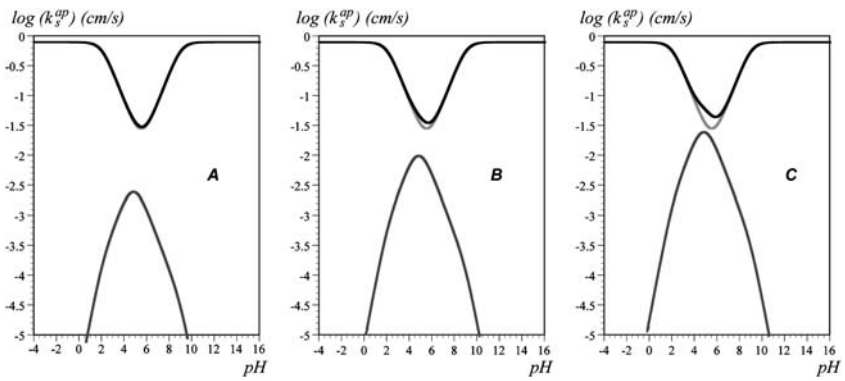

Fig. 3 Variation of the apparent standard rate constant with pH, as a function of the buffer concentration (A: 0.5 M, B: 2 M, C: 5 M; $pK_a = 5$). Black line: apparent standard rate constant, light grey: stepwise pathway contribution, dark grey: concerted pathway contribution. $k_S^X = k_S^{XH} = 0.8$ cm s^{-1} and $k_S^{CEPT}\sqrt{K_{as}^{O+}K_{as}^{R}} = 0.01$ cm s^{-1} M^{-1}; $pK_{X^RH} = 9$ and $pK_{X^OH} = 2$.

importance of the buffer concentration has been previously demonstrated in the oxidation of the $[Os^{II}(bpy)_2py(H_2O)]^{2+}$ complex. The kinetic study of $Os^{II}(OH_2)$/$Os^{III}(OH)$ (sequential process) has revealed an increase of the apparent standard rate constant when the buffer (citric acid, pH 5) concentration is increased up to 2 M.[11] This may indicate a possible contribution of a CPET pathway involving the buffer base as proton acceptor, at the expense of the sequential pathway. Moreover, in the case of the $Os^{III}(OH)/Os^{IV}(O)$ oxidation in 0.1 M Britton–Robinson buffer (boric, citric and phosphoric acids) at a boron-doped diamond electrode, it has been shown that the reaction is fully concerted in the pH range from 4 to 6.5, where the reaction shows a significant kinetic isotope effect, [19] and it was also shown, again as predicted by eqn (4), that increasing the buffer concentration leads to an increase of the oxidation rate constant. In the presence of a buffer, the metal complex is associated to the base within a cluster pair, thus forming weakly bonding adducts as it may be encountered in the active site of proteins. This is the case for example in Photosystem II, [26] within cytochrome c oxidase [8] or superoxide dismutase (SOD), [7] for which prosthetic group surrounding enzymatic active site may play a crucial role in assisting numerous structural modifications related to redox reactions coupled to proton transfer or transport. Such assistance could be provided by weak bonds (*e.g.* hydrogen bonds) with some residue(s), in particular basic residues, and other molecule(s), [27] as *e.g.* water molecules, as it is the case in the active site of FeSOD where one water molecule is present in the H-bond chain of the second sphere residue that allows to transfer protons outside the active site during oxidation of the $Fe^{II}(OH_2)$ complex. [7]

2. Oxidative electrochemistry of a mononuclear Mn^{II} complex in water

As already mentioned, very few analyses exist concerning manganese complexes in spite of the ubiquity of PCET reactions in biological systems. We took as illustrating example the mononuclear complex shown in Fig. 4, whose characteristics and superoxide dismutation properties have been described earlier, [28] with the aim at studying the PCET reaction in water of the aqua-Mn^{II}/hydroxo-Mn^{III} couple (Scheme 3). Fig. 4 shows the slow scan reversible cyclic voltammograms obtained between pH 6 and 9 with the manganese complex henceforward designated by $[LMn^{II}OH_2]^+$. The apparent standard potential, derived from the midpoint between the anodic and cathodic peak potentials, varies linearly with pH as display in Fig. 4b with a slope that indicates the exchange of one proton per electron. This diagram shows the zones of thermodynamic stability of the Mn^{II}-aqua and Mn^{III}-hydroxo complexes. Reversibility was confirmed by a preparative-scale experiment at pH = 7.5: the cyclic voltammogram after electrolysis was identical to the voltammogram recorded before electrolysis, showing that no irreversible transformation of the oxidation product occurs and thus that the reaction simply consists in the conversion of the Mn^{II}-aqua complex to the Mn^{III}-hydroxo complex by exchange of one electron and one proton. Below pH 6, the phenolic oxygen of the ligand is protonated leading to progressive demetallation and a decrease of the cyclic voltammetry wave, of which shape tends to a plateau (Fig. 5a). This feature can be interpreted in the framework of a CE mechanism (Scheme 4) with the chemical reaction C being deprotonation of the ligand. As pH is decreased this reaction becomes less and less favorable. At some point the wave becomes controlled by the kinetics of the deprotonation step leading to a plateau shape wave (passage from a DE zone to a KE zone, see Fig. S1 in the ESI†). The frontier between the two zones is given by $K_{a,LH^+/L}\sqrt{\frac{RT}{F}\frac{k_{+l}}{v[H^+]}} \simeq 1$

where $K_{a,LH^+/L}$ is the acidic constant of the phenol moiety of the ligand and k_{+l} the rate constant for ligand protonation. Simulation of the voltammograms (Fig. 5b) leads to an estimation of $pK_{a,LH^+/L} = 7.5$ and $k_{+l} = 360\ s^{-1}$. Instability of the complex in acidic media was confirmed by UV-vis experiments (see ESI†). Above pH 9, the

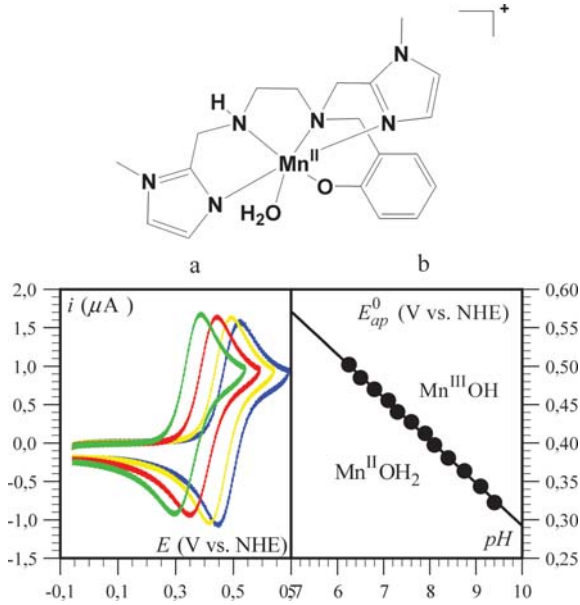

Fig. 4 (a) Slow scan (0.2 V s^{-1}) cyclic voltammogram for the oxidation of 0.8 mM of the above Mn^{II} complex $[LMn^{II}(OH_2)]^+$ in a 0.1 M MES-HEPES-TABS buffer at pH = 6.5 (blue), 7.0 (yellow), 8.1 (red), 9.1 (green). (b) Variation of the apparent standard potential (midpoint between the anodic and cathodic peak potentials) with pH, defining the zones of thermodynamic stability of the Mn^{II}-aqua and Mn^{III}-hydroxo complexes.

wave becomes irreversible and a second wave appears, presumably caused by a dimerization reaction.[20] The possible deprotonation of the secondary amine function of the ligand was ruled out by identical observations made on a similar Mn(II) complex prepared with the methylated ligand (methylation of the secondary amine moiety). Starting from these first results, a preliminary kinetic analysis was then performed in the pH range 6–9.

This kinetic analysis was based on the deviation from the reversible Nernstian behavior displayed in Fig. 4a upon raising the scan rate. It shows the "trumpet plots" formed by the variations of the anodic and cathodic peak potentials with scan rate (Fig. 6), allowing the estimation of an apparent standard rate constant, k_S^{ap}, based on the following Butler–Volmer equation, similar to eqn (3):

$$\frac{I}{F} = k_S^{ap} \exp\left[\frac{F}{2RT}\left(E - E^0_{ap}\right)\right]\left(\sum [Mn^{II}] - \sum [Mn^{III}] \exp\left[-\frac{F}{RT}\left(E - E^0_{ap}\right)\right]\right)$$

relating the current density, I, to the electrode potential, E, where the abovementioned apparent standard potential, E^0_{ap}, is defined by means of the Nernst law:

$$E = E^0_{ap} + \frac{RT}{F}\ln\left(\frac{\sum [Mn^{III}]_{eq}}{\sum [Mn^{II}]_{eq}}\right)$$

$\sum$ indicates a summation of the concentrations *at the electrode surface* over all species having the same oxidation degree. The resulting experimental values of k_S^{ap} (Table 1) show some scatter of the data points, and the precision on *log* k_S^{ap} can be estimated as ± 0.3. No trends in the *log* $k_S^{ap} = f$(pH) variation can be observed.

At first sight, the data are not compatible with stepwise mechanisms (EPT or PET) because a monotonous variation of the rate apparent rate constant is expected for

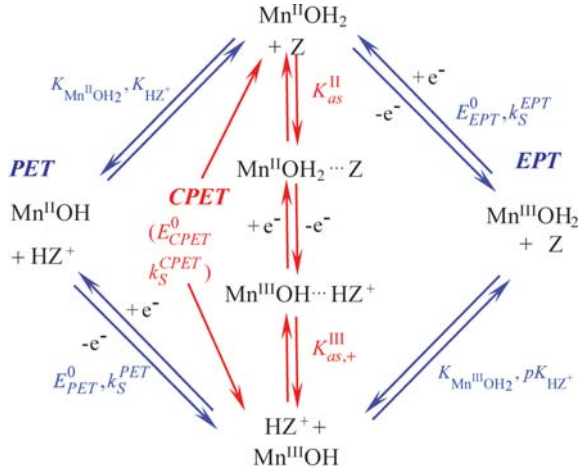

HZ⁺/ Z (charge not shown) is any electroinactive acid-base couple present in the solution including the H_3O^+/H_2O and H_2O /OH^- couples when the solvent is water. $E^0 s$: standard potentials, k_S s: standard rate constants, K s: acid dissociation constants.

Scheme 3 Pathways for PCET oxidation of manganese complex $[LMn^{II}(OH_2)]^+$.

both mechanisms as function of pH (with a slope of ±0.5). However, similar experiments carried out in heavy water produced data points buried in the light water data points, resulting in an undetectable H/D isotopic effect. When the buffer concentration is increased at fixed pH (7.5) from 0.01 M to 1 M, no significant deviation of the voltammograms is observed. Following the criteria recalled in section 1, these experiments rule out a fully concerted mechanism. Moreover, it has to be emphasised that when the scan rate is increased, the cathodic wave does not exactly follow the behavior expected for an simple slow apparent monoelectronic transfer, making the determination of an apparent standard rate constant uncertain (see Fig. 6 for anodic peak potentials and ESI† for voltammograms). This observation can be an

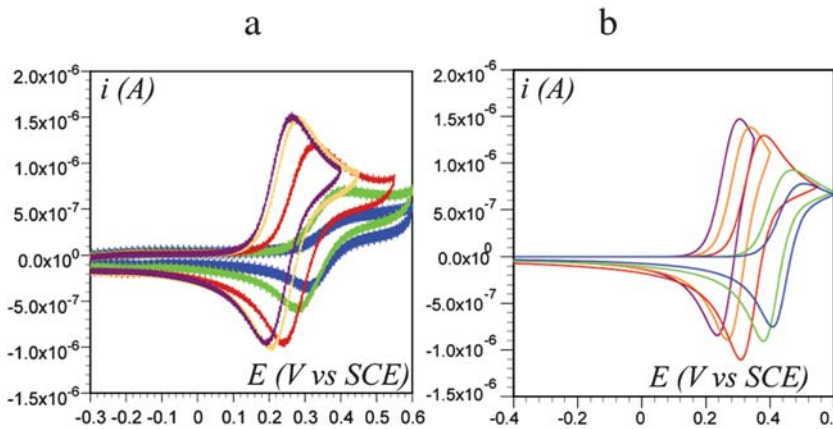

Fig. 5 (a) Slow scan (0.2 V s^{-1}) cyclic voltammograms for the oxidation of 0.8 mM of the Mn^{II} complex $[LMn^{II}(OH_2)]^+$ in a 0.1 M MES-HEPES-TABS buffer at pH 5.1 (blue), pH 5.4 (green), pH 6 (red), pH 6.5 (orange), pH 6.8 (magenta). (b) Simulations (using DigiElch Software[29]).

$$(PhOH)\cdots Mn^{II}LNH(H_2O) \underset{k_{+1}}{\overset{k_{-1}}{\rightleftharpoons}} (PhO)Mn^{II}LNH(H_2O) + H^+$$

$$(PhO)Mn^{II}LNH(H_2O) \overset{E^0_{app}}{\rightleftharpoons} (PhO)Mn^{III}LNH(OH) + e^- + H^+$$

Scheme 4 Mechanism involved for oxidation of manganese complex $[LMn^{II}(OH_2)]^+$ in acidic medium (pH < 6).

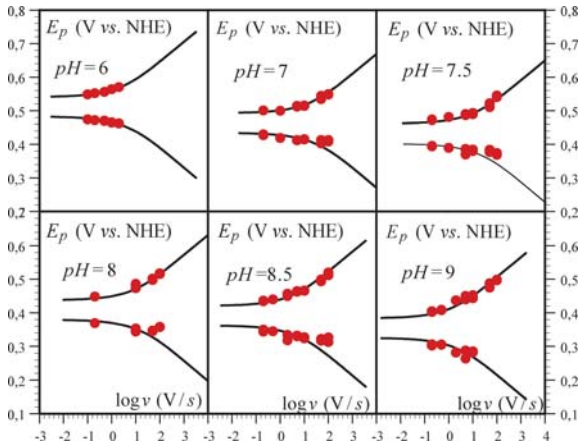

Fig. 6 Cyclic voltammetry of $[LMn^{II}(OH_2)]^+$ in 0.1 M MES-HEPES-TABS buffer as a function of pH and scan rate. "Trumpet plots" (peak potentials, anodic on top, cathodic on bottom) allowing the determination of the apparent standard rate constants by adjustment of the working curves (full lines) to the experimental data (dots) in the framework of a Butler–Volmer rate law with a 0.5 transfer coefficient (see text).

explanation for the lack of a trend in the log $k_S^{ap} = f(\text{pH})$ variation. In that context, we may propose that the observed data could suggest a stepwise pathway (EPT) with fast electron transfer and proton transfer slightly deviating from equilibrium as pH increases. Intervention of PET pathway and concerted pathways cannot be completely excluded. This study points out the difficulty to get mechanistic information when thermodynamical data are lacking. Therefore a strategy involving the attachment of the complex onto the electrode surface to minimize further chemical steps such as dimerization is envisioned so as to expand the investigated pH range.

Concluding remarks

The electro-oxidation studies of water bound Os^{II} complexes provided us with various examples of concerted and stepwise proton-coupled electron transfer reactions. In particular, it has been shown that the conversion of Os^{III}-hydroxo into Os^{IV}-oxo species follows a concerted pathway, despite slower intrinsic kinetics as compared to Os^{II} oxidation, because of the large pK_a gap between the reduced and oxidized species which favored a pathway that avoids intermediates. Such reaction was made possible by the presence of large buffer concentration, which plays the role of proton accepting site within pre-associated weakly bonded adducts. In contrast, Os^{II}-aqua complexes are oxidized along sequential pathways at every pH. These guidelines give the main clues for further studies of biomimicking metal-aqua complexes. We have also shown here that the conditions allowing the assumption commonly made for PCET processes in buffered aqueous media that

Table 1 Apparent standard rate constant, k_S^{ap}, as a function of pH for oxidation of $[LMn^{II}OH_2]^+$

pH	6.5	7	7.5	8	8.5	9
log k_S^{ap}/cm s^{-1}	−1.9	−2.2	−1.95	−2.0	−2.05	−2.1

all acid–base reactions remain at equilibrium are not always met and should be considered in the kinetics analysis of PCET reactions. These criteria apply for other metal complexes mimicking the catalytic site of important biological catalytic processes, like *e.g.* manganese complexes involved in the oxidation of water to oxygen (PSII) or those involved in the dismutation of superoxide anion into oxygen and hydrogen peroxide (Fe- and Mn-superoxide dismutase), or copper complexes acting in cytochrome c oxidase.

The experimental data reported in the present work for a Mn^{II}-aqua/Mn^{III}-hydroxo couple mimicking a Mn-SOD complex did not allow us to draw a clear conclusion regarding the mechanism involved in the studied proton-coupled electron transfer reaction. Nevertheless this preliminary study points out the difficulties to get mechanistic information when thermodynamical data are lacking and allow us to draw a strategy for the choice of a complex with a coordination sphere that favors high stability over a large pH range and prevents additional chemical steps such as dimerization.

Acknowledgements

Partial financial support from the Agence Nationale de la Recherche (Programme Blanc PROTOCOLE) is gratefully acknowledged.

References

1 R. I. Cukier and D. G. Nocera, *Annu. Rev. Phys. Chem.*, 1998, **49**, 337.
2 B. Kok, B. Forbush and M. McGloin, *Photochem. Photobiol.*, 1970, **11**, 457.
3 A. W. Rutherford and A. Boussac, *Science*, 2004, **303**, 1782.
4 T. J. Meyer, M. H. V. Huynh and H. H. Thorp, *Angew. Chem., Int. Ed.*, 2007, **46**, 5284.
5 A.-F. Miller, K. Padmakumar, D. L. Sorkin, A. Karapetian and C. K. Vance, *J. Inorg. Biochem.*, 2003, **93**, 71.
6 A.-F. Miller, *Curr. Opin. Chem. Biol.*, 2004, **8**, 162.
7 A.-F. Miller, *Acc. Chem. Res.*, 2008, **41**, 501.
8 J. P. Collman, N. K. Devaraj, R. A. Decreau, Y. Yang, Y.-L. Yan, W. Ebina, T. A. Eberspacher and C. E. D. Chidsey, *Science*, 2007, **315**, 1565.
9 C. Costentin, M. Robert and J.-M. Savéant, *Acc. Chem. Res.*, 2010, **43**, 1019.
10 C. Costentin, M. Robert and J.-M. Savéant, *J. Am. Chem. Soc.*, 2007, **129**, 9953.
11 C. Costentin, M. Robert, J.-M. Savéant and A.-L. Teillout, *ChemPhysChem*, 2009, **10**, 191.
12 M. H. V. Huynh and T. J. Meyer, *Chem. Rev.*, 2007, **107**, 5004.
13 S. J. Slattery, J. K. Blaho, J. Lehnes and K. A. Goldsby, *Coord. Chem. Rev.*, 1998, **174**, 391.
14 K. J. Takeuchi, M. S. Thompson, D. W. Pipes and T. J. Meyer, *Inorg. Chem.*, 1984, **23**, 1845.
15 R. A. Binstead and T. J. Meyer, *J. Am. Chem. Soc.*, 1987, **109**, 3287.
16 R. A. Binstead, B. A. Moyer, G. J. Samuels and T. J. Meyer, *J. Am. Chem. Soc.*, 1981, **103**, 2897.
17 R. M. Haddox and H. O. Finklea, *J. Phys. Chem. B*, 2004, **108**, 1694.
18 N. Madhiri and H. O. Finklea, *Langmuir*, 2006, **22**, 10643.
19 C. Costentin, M. Robert, J.-M. Savéant and A.-L. Teillout, *Proc. Natl. Acad. Sci. U. S. A.*, 2009, **106**, 11829.
20 M.-N. Collomb and A. Deronzier, *Eur. J. Inorg. Chem.*, 2009, 2025.

21 C. Hureau, G. Blondin, M.-F. Charlot, C. Philouze, M. Nierlich, M. Césario and E. Anxolabéhère-Mallart, *Inorg. Chem.*, 2005, **44**, 3669.
22 C. Hureau, L. Sabater, E. Anxolabéhère-Mallart, M. Nierlich, M.-F. Charlot, F. Gonnet, E. Rivière and G. Blondin, *Chem.–Eur. J.*, 2004, **10**, 1998.
23 H. H. Thorp, G. W. Brudvig and E. F. Bowden, *J. Electroanal. Chem.*, 1990, **290**, 293.
24 E. Vianello and J-M. Savéant, *Electrochim. Acta*, 1963, **8**, 905.
25 L. Nadjo and J-M. Savéant, *J. Electroanal. Chem.*, 1973, **48**, 113.
26 W. Lubitz, E. J. Reijerse and J. Messinger, *Energy Environ. Sci.*, 2008, **1**, 15.
27 A. Guskov, J. Kern, A. Gabdulkhakov, M. Broser, A. Zouni and W. Saenger, *Nat. Struct. Mol. Biol.*, 2009, **16**, 334.
28 F. Cisnetti, A.-S. Lefèvre, R. Guillot, F. Lambert, G. Blain, E. Anxolabéhère-Mallart and C. Policar, *Eur. J. Inorg. Chem.*, 2007, 4472.
29 M. Rudolph, *J. Electroanal. Chem.*, 2003, **543**, 23.